

## Enhanced optical absorption and photocatalytic activity of anatase TiO<sub>2</sub> through (Si,Ni) codoping

Yanming Lin, Zhenyi Jiang, Chaoyuan Zhu, Xiaoyun Hu, Xiaodong Zhang, Haiyan Zhu, and Jun Fan

Citation: *Applied Physics Letters* **101**, 062106 (2012); doi: 10.1063/1.4745193

View online: <http://dx.doi.org/10.1063/1.4745193>

View Table of Contents: <http://scitation.aip.org/content/aip/journal/apl/101/6?ver=pdfcov>

Published by the *AIP Publishing*

---

### Articles you may be interested in

Synergistic effect of V/N codoping by ion implantation on the electronic and optical properties of TiO<sub>2</sub>  
*J. Appl. Phys.* **115**, 143106 (2014); 10.1063/1.4871192

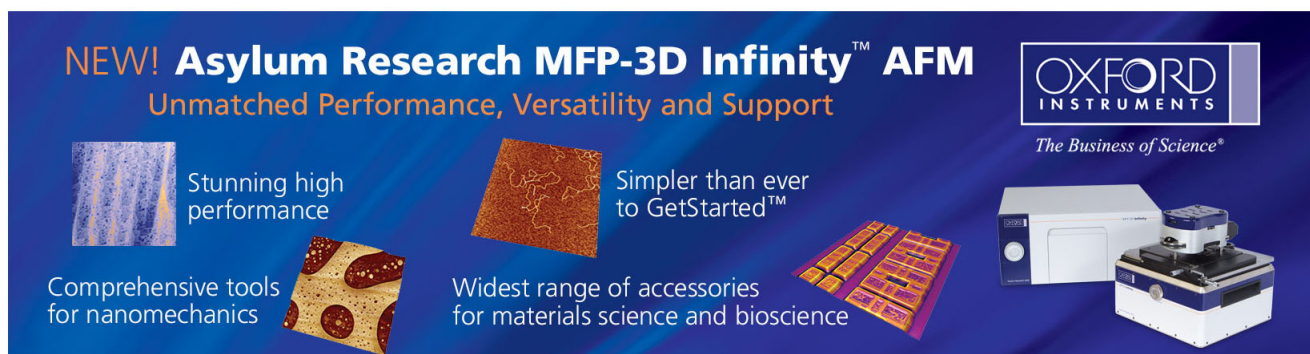
Cationic (V, Y)-codoped TiO<sub>2</sub> with enhanced visible light induced photocatalytic activity: A combined experimental and theoretical study  
*J. Appl. Phys.* **114**, 183514 (2013); 10.1063/1.4831658

Enhancement of optical absorption by modulation of the oxygen flow of TiO<sub>2</sub> films deposited by reactive sputtering  
*J. Appl. Phys.* **111**, 113513 (2012); 10.1063/1.4724334

The electronic and optical properties of Eu/Si-codoped anatase TiO<sub>2</sub> photocatalyst  
*Appl. Phys. Lett.* **100**, 102105 (2012); 10.1063/1.3692750

Enhanced visible-light photocatalytic activity of anatase TiO<sub>2</sub> through N and S codoping  
*Appl. Phys. Lett.* **98**, 211903 (2011); 10.1063/1.3593147

---



**NEW! Asylum Research MFP-3D Infinity™ AFM**  
Unmatched Performance, Versatility and Support

**OXFORD INSTRUMENTS**  
*The Business of Science®*

Stunning high performance  
Simpler than ever to GetStarted™  
Comprehensive tools for nanomechanics  
Widest range of accessories for materials science and bioscience

The advertisement features several images: a blue textured surface, a brown textured surface, a grid of colorful rectangular samples, and the Asylum Research MFP-3D Infinity AFM instrument.

## Enhanced optical absorption and photocatalytic activity of anatase TiO<sub>2</sub> through (Si,Ni) codoping

Yanming Lin,<sup>1,a)</sup> Zhenyi Jiang,<sup>1,b)</sup> Chaoyuan Zhu,<sup>2</sup> Xiaoyun Hu,<sup>3</sup> Xiaodong Zhang,<sup>1</sup> Haiyan Zhu,<sup>1</sup> and Jun Fan<sup>4</sup>

<sup>1</sup>Institute of Modern Physics, Northwest University, Xi'an 710069, People's Republic of China

<sup>2</sup>Department of Applied Chemistry, Institute of Molecular Science and Center for Interdisciplinary Molecular Science, National Chiao-Tung University, Hsinchu 30050, Taiwan

<sup>3</sup>Department of Physics, Northwest University, Xi'an 710069, People's Republic of China

<sup>4</sup>School of Chemical Engineering, Northwest University, Xi'an 710069, People's Republic of China

(Received 2 April 2012; accepted 27 July 2012; published online 9 August 2012)

The electronic and optical properties of (Si,Ni)-codoped anatase TiO<sub>2</sub> are investigated using the density functional theory. The calculated results indicate that the synergistic effects of (Si,Ni) codoping can effectively extend the optical absorption edge, which can lead to higher visible-light photocatalytic activity than pure anatase TiO<sub>2</sub>. To verify the reliability of our calculated results, nanocrystalline (Si,Ni)-codoped TiO<sub>2</sub> is synthesized by a sol-gel-solvothermal method, and experimental results also show that the (Si,Ni)-codoped sample exhibits better absorption performance and higher photocatalytic activities than pure TiO<sub>2</sub>. © 2012 American Institute of Physics. [<http://dx.doi.org/10.1063/1.4745193>]

Titania (TiO<sub>2</sub>) has received intense attention as a promising candidate material for solar energy conversion and photocatalyst applications.<sup>1,2</sup> However, the universal applications of TiO<sub>2</sub> are restricted to ultraviolet (UV) light ( $\lambda < 385$  nm) due to the wide band gap of anatase TiO<sub>2</sub> ( $\sim 3.2$  eV). Therefore, reducing the band gap of anatase TiO<sub>2</sub> to make it photosensitive to visible-light has become one of the most important goals in photocatalytic applications. It has been suggested that doping with C, N, S, and Ni would result in a reduced band gap for TiO<sub>2</sub>.<sup>3-5</sup>

A few latest researches show that different ions codoping into TiO<sub>2</sub> can further narrow its band gap and enhance its photocatalytic activity.<sup>6-13</sup> For example, Li *et al.* reported the C/H-codoping produces significant bandgap narrowing, which leads to higher visible-light photocatalytic efficiency than the C-doped anatase TiO<sub>2</sub>.<sup>8</sup> The research of Su *et al.* suggested that the codoping of TiO<sub>2</sub> with N and Fe leads to the much narrowing of the band gap and greatly improves the photocatalytic activity under visible-light irradiation.<sup>9</sup> These results indicate that codoping is one of the most effective approaches to extend the absorption edge to the visible-light range in anatase TiO<sub>2</sub>. However, photocatalytic activity and optical absorption properties of (Si,Ni)-codoped TiO<sub>2</sub> have no report on the theory and experiment. Thus, the enhanced optical absorption and photocatalytic activity are expected for (Si,Ni)-codoped TiO<sub>2</sub>.

In this letter, the electronic and optical properties of (Si,Ni)-codoped TiO<sub>2</sub> were investigated based on the density functional theory (DFT) to reveal the synergistic effects of (Si,Ni) codoping on the mechanism of band gap reducing and origin of the enhanced visible-light photocatalytic activity. Nanocrystalline (Si,Ni)-codoped TiO<sub>2</sub> was synthesized by sol-gel-solvothermal method. It was found that the

(Si,Ni)-codoped TiO<sub>2</sub> showed excellent photocatalytic activity for the degradation of methylene blue (MB), which verified the reliability of our calculation.

All the spin-polarized calculations were performed using the projector augmented wave pseudopotentials as implemented in the VASP code.<sup>14,15</sup> The exchange correlation function was treated by the generalized gradient approximation (GGA) with the Perdew-Wang parameterization (known as GGA-PW91).<sup>16</sup> A cutoff energy of 500 eV and a Monkhorst-Pack *k*-point mesh<sup>17</sup> of  $9 \times 9 \times 9$  was used for geometry optimization, electronic, and optical properties calculations. Using the block Davidson scheme, both the atomic positions and cell parameters were optimized until the residual forces were below 0.01 eV/Å. It is well-known that the traditional DFT method usually underestimates the band gap for semiconductors. However, the DFT+*U* approach introduces an on-site correction in order to describe systems with localized *d* electron, which can produce better band gaps in comparison with experimental results. Therefore, our all calculations of the electronic and the optical properties were conducted using the GGA+*U* method<sup>18-21</sup> for both Ti 3*d* and Ni 3*d* electrons. It was found that the band gap of pure anatase TiO<sub>2</sub> was 2.9 eV with *U* = 10.0 eV and *J* = 1.0 eV for Ti 3*d* electrons and was only weakly dependent on *J* value. This accords well with the experimental value of 3.2 eV.<sup>22</sup>

The valence electron configurations considered in this study included Ti (3*d*<sup>2</sup>4*s*<sup>2</sup>), O (2*s*<sup>2</sup>2*p*<sup>4</sup>), Si (3*s*<sup>2</sup>3*p*<sup>2</sup>), and Ni (3*d*<sup>8</sup>4*s*<sup>2</sup>). All the doped systems were constructed from a relaxed (2 × 2 × 1) 48-atom anatase TiO<sub>2</sub> supercell, shown in Fig. 1(a). As the position of Ni in the TiO<sub>2</sub> lattice was unclear, variety of positions of Ni atoms in the lattice were considered, such as substitutional Ni at the Ti site (Ni@Ti) and O site (Ni@O). Theoretical results confirmed that Si atom was incorporated as cation in the TiO<sub>2</sub> lattice, an Ti atom was substituted by an Si atom (Si@Ti).<sup>23</sup> Similar substitutions were also considered for codoped systems, as Si locates at Ti site and Ni locates at either Ti or O site

<sup>a)</sup>Electronic mail: linyminwu@gmail.com.

<sup>b)</sup>Author to whom correspondence should be addressed. Electronic mail: jiangzy@nwu.edu.cn. Tel.: 86-29-88303491. Fax: 86-29-88302331.

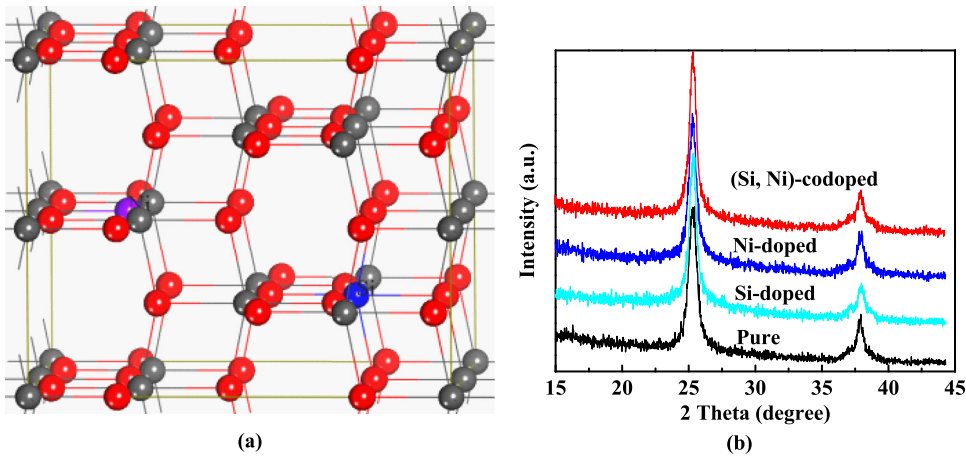


FIG. 1. (a) 48-atom supercell model for defective anatase  $\text{TiO}_2$  shows the location of the dopants. The atom doping sites are marked with Si and Ni. The gray spheres and red spheres represent the Ti and O atoms, respectively. The blue sphere and purple sphere represent Si and Ni atom, respectively. (b) XRD patterns for the pure and doped  $\text{TiO}_2$ .

( $\text{Si}@Ti\&Ni@Ti$  and  $\text{Si}@Ti\&Ni@O$ ). To determine the relative stabilities of the doped systems, we calculated the defect formation energies ( $E_f$ ) for the monodoped and codoped systems according to the formulas

$$E_{f(X@Y)} = E_{(X@Y)} - E_{(\text{pure})} - (\mu_X - \mu_Y), \quad (1)$$

$$E_{f(\text{Si}@Y\&Ni@Y)} = E_{(\text{Si}@Y\&Ni@Y)} - E_{(\text{pure})} - (\mu_{\text{Si}} + \mu_{\text{Ni}} - \mu_Y - \mu_Y), \quad (2)$$

where  $X = \text{Si}, \text{Ni}$ ,  $Y = \text{Ti}, \text{O}$ ,  $E$  represents the total energy, and  $\mu$  is the chemical potential. The chemical potential of O atom ( $\mu_{\text{O}}$ ) is determined by the energy of an  $\text{O}_2$  molecule. The calculated formation energies are listed in Table I. It shows that Ni impurity is preferred to substitute O in lattice because of the smallest formation energy in both Ni-doped and (Si,Ni)-codoped systems. Moreover, the charge analyses indicate that the impurities atoms of Si and Ni present a positive valance state, which is consistent with the experimental results.

To investigate the electronic properties of Si and/or Ni (co)doping anatase  $\text{TiO}_2$ , the total density of states (TDOS) and partial density of states (PDOS) were plotted in Fig. 2. It shows that the valence band (VB) is dominated by O 2p states while the conduction band (CB) consists mainly of Ti 3d states for pure anatase  $\text{TiO}_2$ . In Si-doped ( $\text{Si}@Ti$ )  $\text{TiO}_2$ , the CB broadens with the mixing of Ti 3d and Si 3s states, and the CB bottom has a decline about 0.5 eV, which can lead to a band gap narrowing. For Ni-doped ( $\text{Ni}@O$ )  $\text{TiO}_2$ , it can be observed that the band gap decreases by about 0.2 eV and most Ni 3d states are located in the band gap compared with the pure anatase  $\text{TiO}_2$ , which may be due to stronger interactions between the Ni 3d and O 2p orbitals. For (Si,Ni)-codoped ( $\text{Si}@Ti\&Ni@O$ )  $\text{TiO}_2$ , a series of impurity states (Ni 3d) appear in the band gap, and all of impurity energy levels are located above the valence band maximum and below the conduction band minimum. Moreover, the

band gap narrowed by 0.5 eV compared with the pure anatase  $\text{TiO}_2$ . Therefore, synergistic effect of (Si,Ni) codoping can lead to a decrease of the photon excitation energy and shift the optical absorption edge to the visible-light region.

It is well-known that optical absorption is a surface property in anatase  $\text{TiO}_2$ . However, it is reasonable that the effect of doping on electronic structure and optical absorption properties of anatase  $\text{TiO}_2$  are investigated by the bulk anatase  $\text{TiO}_2$ ,<sup>24–26</sup> which partially reflects some experimental results. According to the obtained electronic structures, we calculated the complex dielectric function  $\xi = \xi_1 + i\xi_2$ . The corresponding absorption spectrum was estimated by the following equation:

$$I(\omega) = 2\omega \left( \frac{(\xi_1^2(\omega) + \xi_2^2(\omega))^{1/2} - \xi_1(\omega)}{2} \right)^{1/2}, \quad (3)$$

where  $I$  is the optical absorption coefficient and  $\omega$  is the angular frequency ( $E = \hbar\omega$ ).

The optical absorption spectrum of the pure and doped systems is calculated, as shown in Fig. 3. It is found that pure anatase  $\text{TiO}_2$  can only respond to the ultraviolet (UV) light and shows no absorption activity in the visible-light region. For Si-doped ( $\text{Si}@Ti$ )  $\text{TiO}_2$ , it is clear that the narrowed band gap induces the increasing optical absorption in the UV-light region. For Ni-doped ( $\text{Ni}@O$ )  $\text{TiO}_2$ , there are a series of impurity states (Ni 3d orbital) appearing in the forbidden gap, which leads to a more significant the absorption of visible-light. For (Si,Ni)-codoped ( $\text{Si}@Ti\&Ni@O$ )  $\text{TiO}_2$  system, synergistic effect of (Si,Ni) codoping induces a band gap narrowing and a series of impurity states appearing in the band gap, which can lead to a decrease of the photon excitation energy in the view of electronic structure. Therefore, the absorption of UV- and visible-light are greatly enhanced, and there is a large visible-light absorption wave packet at  $600 \pm 50$  nm, which may be responsible for the outstanding photocatalytic activity and the red-shift of optical absorption edge in (Si,Ni)-codoped anatase  $\text{TiO}_2$ .

In order to confirm the better photocatalytic activity of the (Si,Ni)-codoped  $\text{TiO}_2$  compared to that of pure  $\text{TiO}_2$ , we further observed the UV-vis absorption spectrum by experiments.

Nanocrystalline pure, Si-, Ni-, and (Si,Ni)-codoped  $\text{TiO}_2$  were synthesized by a sol-gel-solvothermal method.

TABLE I. Defect formation energies  $E_f$  for different doped anatase  $\text{TiO}_2$  systems.

Doped models	Si@Ti	Ni@Ti	Ni@O	Si@Ti&Ni@Ti	Si@Ti&Ni@O
$E_f$ (eV)	1.6452	8.0914	2.6591	9.6748	2.8120

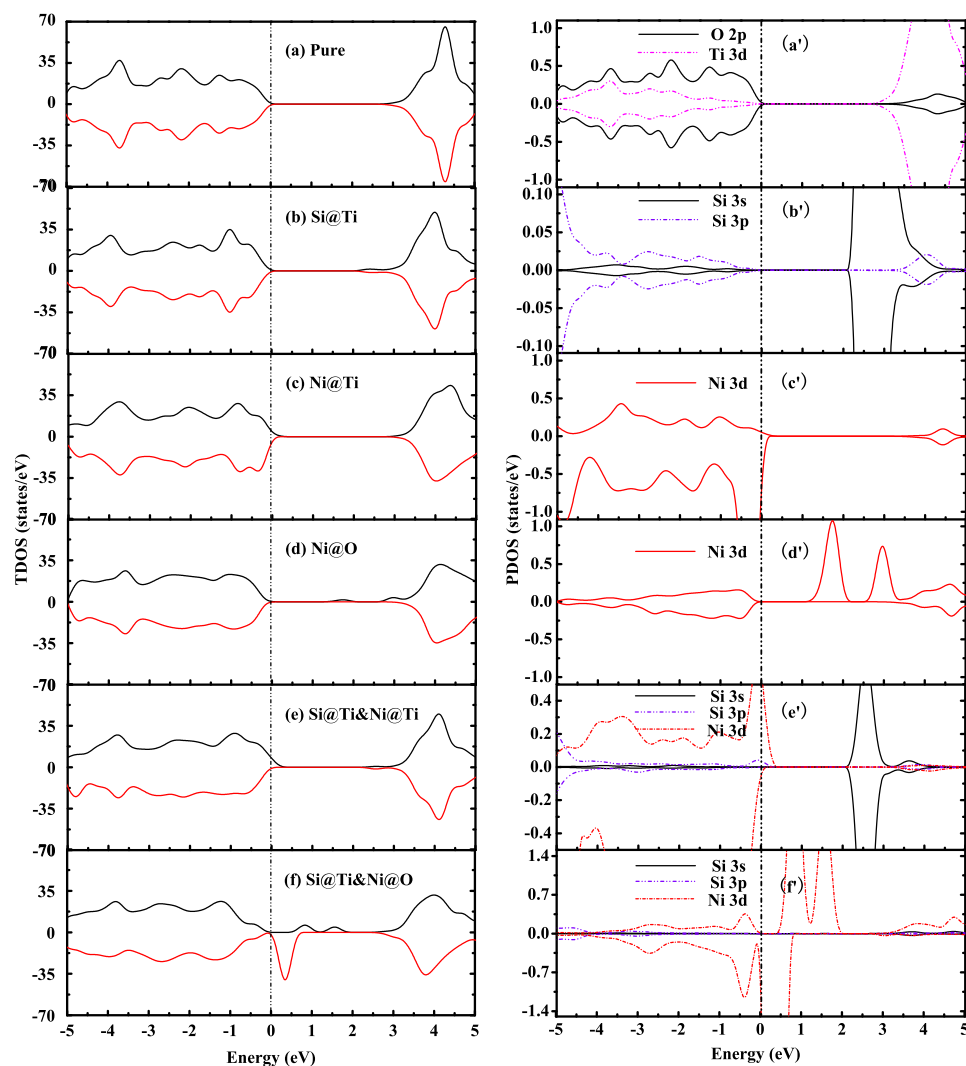


FIG. 2. Calculated TDOS and PDOS of different doped  $\text{TiO}_2$ . The top of the valence band of pure anatase  $\text{TiO}_2$  is taken as the reference level.

Firstly, a desired amount (0.1938 g) of nickel nitrate hexahydrate was dissolved in 31.70 mL of glacial acetic acid solution under stirring. Then, 7.44 mL of tetraethyl orthosilicate was dropwise added into the solution with stirring for 1 h. Second, 22.69 mL of Tetrabutyl titanate was also dropwise added into the solution with continuous stirring for 2 h, and the solution was heated in an oven and kept at  $140^\circ\text{C}$  for 14 h. Finally, the precipitate obtained was dried in a vacuum oven at  $70^\circ\text{C}$  for 48 h. To evaluate the photocatalytic activity of samples, photocatalytic experiments were

carried out in an inner-irradiation-type reactor, and a 500 W long-arc xenon lamp was used as the simulated solar light source.

The crystalline phase was identified by x-ray diffraction (XRD) (Rigaku D/MAX-2400). The Brunauer-Emmett-Teller (BET) surface area of the samples was measured through nitrogen adsorption at 77 K (Nova 2000 e). The UV-vis absorption spectra were obtained using an UV-vis spectrophotometer (UV-3600) and using  $\text{BaSO}_4$  as the reference sample.

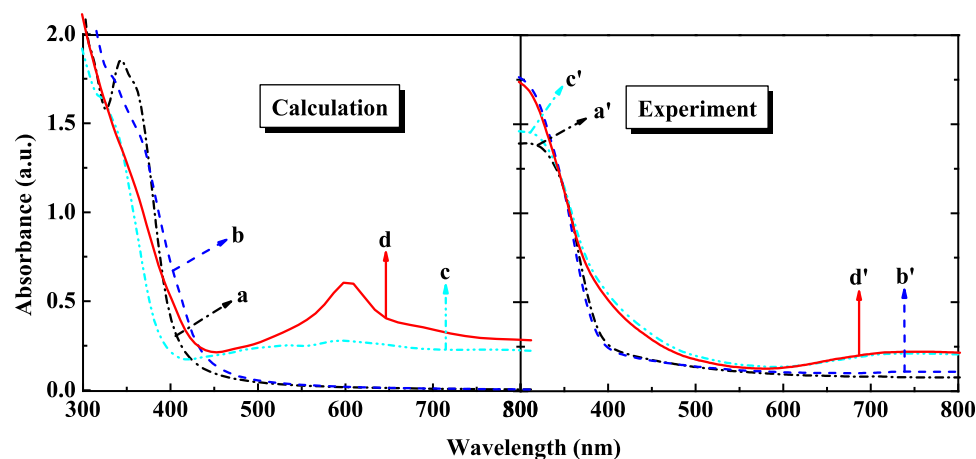


FIG. 3. The optical absorption curves of (a, a') pure, (b, d') Si-doped, (c, c') Ni-doped, (d, d') (Si,Ni)-codoped  $\text{TiO}_2$ . The left and right figures represent the absorption spectra obtained by calculations and experiments, respectively.



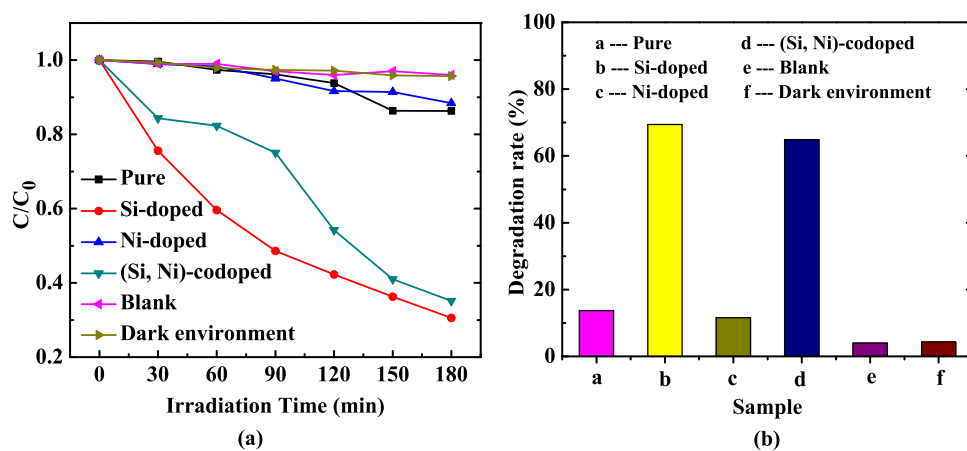


FIG. 4. Photocatalytic degradation rate of MB test during irradiation with visible-light radiation: (a) MB concentration changes as a function of irradiation time, and (b) the comparison of degradation rate after 3 h of visible-light radiation.

Fig. 1(b) shows the XRD patterns of the samples of pure, Si-, Ni-, and (Si,Ni)-codoped  $\text{TiO}_2$ . It is found that all of the diffraction peaks are contributed by the anatase  $\text{TiO}_2$  phase and no other visible impurity peak can be distinguished in the pattern of pure or doped sample. The BET surface areas for pure, Si-, Ni-, and (Si,Ni)-codoped  $\text{TiO}_2$  are 84.33, 252.31, 224.52, and 321.20  $\text{m}^2/\text{g}$ , respectively. Obviously, with the coexistence of Si and Ni in  $\text{TiO}_2$ , the surface area of  $\text{TiO}_2$  powders is increased to 321.20  $\text{m}^2/\text{g}$ , about four times of that of pure  $\text{TiO}_2$  powders.

The optical absorption spectra of the pure and doped systems are obtained by experiments, shown in Fig. 3. Compared with the pure  $\text{TiO}_2$ , it is clear that the incorporation of Si into  $\text{TiO}_2$  lattice induces the enhanced optical absorption in the UV-light region. For Ni-doped system, it shows good absorption activity in the visible-light region. For (Si,Ni)-codoped  $\text{TiO}_2$  system, the optical absorption curve shows that codoped  $\text{TiO}_2$  with Si and Ni can greatly enhance the absorption of UV- and visible-light, which indicates synergistic effect of (Si,Ni) codoping. However, there are some misalignments between the experimental and theoretical results. In particular, there is a disparity between the DFT codoped results at 600 nm with experiment, which may be due to the shortcomings of the DFT leading to an unfaithful prediction for the impurity state. But, from the perspective of qualitative analysis, the experimental results are consistent with the calculations.

The photocatalytic activity of the pure and doped samples were evaluated by monitoring the degradation of MB, as shown in Fig. 4. The “Dark environment” shows that MB almost cannot be degraded using catalysts without the visible-light irradiation. The “Blank” shows that MB almost cannot be degraded under the visible-light irradiation without catalysts, indicating that the photolysis can be ignored. The Si-doped sample presents the best photocatalytic activity while the degradation rate of  $\text{TiO}_2$  is reduced after doping with Ni. This is because the impurity states of Ni 3d is also easy to become the recombination center of electron-hole pairs. For (Si,Ni)-codoped  $\text{TiO}_2$  sample (see Fig. 4), the improvement of photocatalytic activity in the codoping sample can be attributed to the enhanced absorption of UV- and visible-light. Therefore, the (Si,Ni)-codoped sample exhibits better photocatalytic activity than the pure and Ni-doped sample, lower than the Si-doped sample.

In summary, we have studied the electronic and optical properties of (Si,Ni)-codoped  $\text{TiO}_2$  based on DFT calculations. The synergistic effects of (Si,Ni) codoping may further reduce the electrons excited energy from VB to CB under the visible-light irradiation, which enhances the photocatalytic activity and the red-shift of absorption edge. The photocatalytic and optical absorption properties obtained by experiments reveal that (Si,Ni)-codoped  $\text{TiO}_2$  has a much stronger absorption and photocatalytic activity than the pure  $\text{TiO}_2$ , which verifies the reliability of the calculation results.

This work was supported by the National Science Foundation of China under Grants (Nos. 10647008, 50971099, 20876125, and 21176199), the Research Fund for the Doctoral Program of Higher Education (Nos. 20096101110017 and 20096101110013), Key Project of Natural Science Foundation of Shaanxi Province of China (Nos. 2010JZ002 and 2011JM1001). Yanming Lin would like to thank Dr. Kesong Yang and Dr. Run Long for helpful discussions on the topic.

<sup>1</sup>A. Fujishima and K. Honda, *Nature (London)* **238**, 37 (1972).

<sup>2</sup>T. D. Beeson and D. W. C. MacMillan, *J. Am. Chem. Soc.* **127**, 8826 (2005).

<sup>3</sup>R. Asahi, T. Morikawa, T. Ohwaki, K. Aoki, and Y. Taga, *Science* **293**, 269 (2001).

<sup>4</sup>S. U. M. Khan, M. Al-Shahry, and W. B. Ingler, Jr., *Science* **297**, 2243 (2002).

<sup>5</sup>Y. M. Lin, Z. Y. Jiang, C. Y. Zhu, X. Y. Hu, X. D. Zhang, and J. Fan, *Mater. Chem. Phys.* **133**, 746 (2012).

<sup>6</sup>L. Jia, C. Wu, Y. Li, S. Han, Z. Li, B. Chi, J. Pu, and L. Jian, *Appl. Phys. Lett.* **98**, 211903 (2011).

<sup>7</sup>R. Long and N. J. English, *Chem. Mater.* **22**, 1616 (2010).

<sup>8</sup>N. Li, K. L. Yao, L. Li, Z. Y. Sun, G. Y. Gao, and L. Zhu, *J. Appl. Phys.* **110**, 073513 (2011).

<sup>9</sup>Y. Su, Y. Xiao, Y. Li, Y. Du, and Y. Zhang, *Mater. Chem. Phys.* **126**, 761 (2011).

<sup>10</sup>P. P. González-Borrero, H. S. Bernabé, N. G. C. Astrath, A. C. Bento, M. L. Baesso, M. V. Castro Meira, J. S. De Almeida, and A. Ferreira da Silva, *Appl. Phys. Lett.* **99**, 221909 (2011).

<sup>11</sup>Y. M. Lin, Z. Y. Jiang, X. Y. Hu, X. D. Zhang, J. Fan, H. Miao, and Y. B. Shang, *Chin. Phys. B* **21**, 033103 (2012).

<sup>12</sup>G. G. Nakhate, V. S. Nikam, K. G. Kanade, S. Arbuji, B. B. Kale, and J. O. Baeg, *Mater. Chem. Phys.* **124**, 976 (2010).

<sup>13</sup>D. Zhao, X. Huang, B. Tian, S. Zhou, Y. Li, and Z. Du, *Appl. Phys. Lett.* **98**, 162107 (2011).

<sup>14</sup>G. Kresse and J. Hafner, *Phys. Rev. B* **47**, 558 (1993).

<sup>15</sup>G. Kresse and J. Furthemüller, *Phys. Rev. B* **54**, 11169 (1996).

<sup>16</sup>J. P. Perdew, S. Burke, and M. Ernzerhof, *Phys. Rev. Lett.* **77**, 3865 (1996).

<sup>17</sup>H. J. Monkhorst and J. D. Pack, *Phys. Rev. B* **13**, 5188 (1976).

- <sup>18</sup>S. L. Dudarev, G. A. Botton, S. Y. Savarsov, C. J. Humphreys, and A. P. Sutton, *Phys. Rev. B* **57**, 1505 (1998).
- <sup>19</sup>K. Yang, Y. Dai, B. Huang, and Y. P. Feng, *Phys. Rev. B* **81**, 033202 (2010).
- <sup>20</sup>K. Yang, Y. Dai, B. Huang, and M. H. Whangbo, *J. Phys. Chem. C* **113**, 2624 (2009).
- <sup>21</sup>M. E. Arroyo-de Dompablo, A. Morales-Garca, and M. Taravillo, *J. Chem. Phys.* **135**, 054503 (2011).
- <sup>22</sup>H. Tang, F. Lévy, H. Berger, and P. E. Schmid, *Phys. Rev. B* **52**, 7771 (1995).
- <sup>23</sup>K. Yang, Y. Dai, and B. Huang, *Chem. Phys. Lett.* **456**, 71 (2008).
- <sup>24</sup>K. Yang, Y. Dai, and B. Huang, *J. Phys. Chem. C* **111**, 12086 (2007).
- <sup>25</sup>R. Shirley, M. Kraft, and O. R. Inderwildi, *Phys. Rev. B* **81**, 075111 (2010).
- <sup>26</sup>L. Jia, C. Wu, S. Han, N. Yao, Y. Li, Z. Li, B. Chi, J. Pu, and L. Jian, *J. Alloys Compd.* **509**, 6067 (2011).